Article

Spectroscopic Determination of Hydrogenation Rates and Intermediates during Carbonyl Hydrogenation Catalyzed by Shvo's Hydroxycyclopentadienyl Diruthenium Hydride Agrees with Kinetic Modeling Based on Independently Measured Rates of Elementary Reactions

Charles P. Casey, Sharon E. Beetner, and Jeffrey B. Johnson

J. Am. Chem. Soc., **2008**, 130 (7), 2285-2295 • DOI: 10.1021/ja077525c

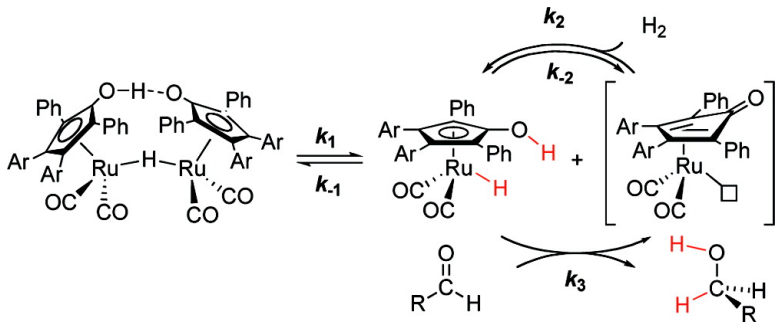

More About This Article

Additional resources and features associated with this article are available within the HTML version:

- Supporting Information
- Links to the 3 articles that cite this article, as of the time of this article download
- Access to high resolution figures
- Links to articles and content related to this article
- Copyright permission to reproduce figures and/or text from this article

View the Full Text HTML

J|A|C|S
ARTICLES
Published on Web 01/24/2008

Spectroscopic Determination of Hydrogenation Rates and Intermediates during Carbonyl Hydrogenation Catalyzed by Shvo's Hydroxycyclopentadienyl Diruthenium Hydride Agrees with Kinetic Modeling Based on Independently Measured Rates of Elementary Reactions

Charles P. Casey,* Sharon E. Beetner, and Jeffrey B. Johnson

Department of Chemistry, University of Wisconsin-Madison, Madison, Wisconsin 53706

Received September 29, 2007; E-mail: casey@chem.wisc.edu

Abstract: The catalytic hydrogenation of benzaldehyde and acetophenone with the Shvo hydrogenation catalysts were monitored by *in situ* IR spectroscopy in both toluene and THF. The disappearance of organic carbonyl compound and the concentrations of the ruthenium species present throughout the hydrogenation reaction were observed. The dependence of the hydrogenation rate on substrate, H_2 pressure, total ruthenium concentration, and solvent were measured. In toluene, bridging diruthenium hydride **1** was the only observable ruthenium species until nearly all of the substrate was consumed. In THF, both **1** and some monoruthenium hydride **2** were observed during the course of the hydrogenation. A full kinetic model of the hydrogenation based on rate constants for individual steps in the catalysis was developed. This kinetic model simulates the rate of carbonyl compound hydrogenation and of the amounts of ruthenium species **1** and **2** present during hydrogenations.

Introduction

Ligand−metal bifunctional hydrogenation catalysis is dramatically changing the face of reduction chemistry.[1] These transition metal catalysts contain electronically coupled hydridic and acidic hydrogens that are transferred to polar unsaturated species under mild conditions. The first such catalyst, Shvo's (hydroxycyclopentadienyl) diruthenium bridging hydride (**1-S**), was developed in the mid 1980s.[2−4] More recently, Noyori has developed a series of chiral ruthenium(diamine)(diphosphine) catalysts, including ruthenium(dpen)(tol-BINAP) (Figure 1), which display extraordinary activity and enantioselectivity in the hydrogenation of a diverse range of ketones.[5]

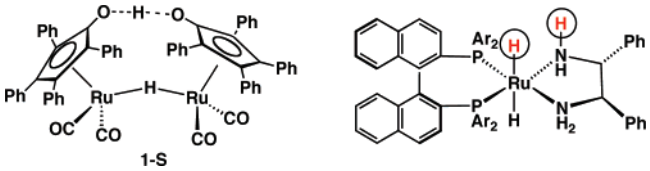

Figure 1. Examples of ligand−metal bifunctional catalysts.

For hydrogenation of aldehydes and ketones, Shvo used the diruthenium bridging hydride as the precatalyst and operated at high temperatures (145 °C) and pressures (35 atm).[2] The bridging diruthenium hydride **1-S** is unreactive for the stoichiometric reduction of aldehydes, whereas the monoruthenium hydride **2-S** rapidly reduces ketones and aldehydes. In 1986, Shvo proposed a catalytic cycle in which the diruthenium bridging hydride reversibly dissociates to monoruthenium hydride **2-S** and a reactive intermediate **A-S** (Scheme 1).[3] Reduction of aldehydes by **2-S** produces an alcohol and the reactive intermediate **A-S**. The reactive intermediate **A-S** reacts with H_2 to regenerate the active reducing agent **2-S**. This working hypoth-

Scheme 1. Catalytic Cycle for the Hydrogenation of Aldehydes with the Shvo Catalyst

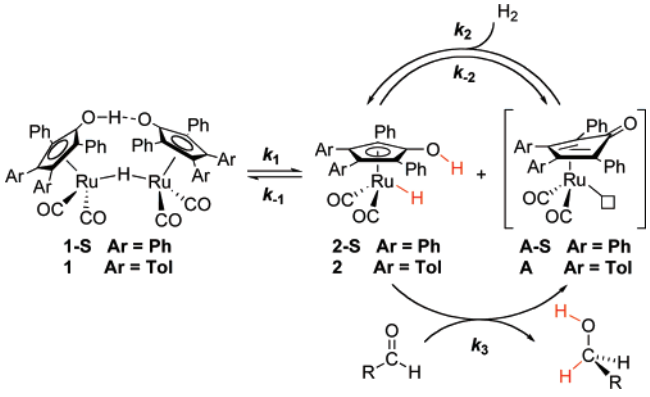

(1) For reviews of ligand-metal bifunctional catalysis, see: (a) Noyori, R.; Ohkuma, T. *Angew. Chem., Int. Ed.* **2001**, *40*, 40−73. (b) Noyori, R.; Kitamura, M.; Ohkuma, T. *Proc. Natl. Acad. Sci. U.S.A.* **2004**, *101*, 5356−5362. (c) Clapham, S. E.; Hadzovic, A.; Morris, R. H. *Coord. Chem. Rev.* **2004**, *248*, 2201−2237. (d) Ikariya, T.; Murata, K.; Noyori, R. *Org. Biomol. Chem.* **2006**, *4*, 393−406.

(2) Blum, Y.; Czarkie, D.; Rahamin, Y.; Shvo, Y. *Organometallics* **1985**, *4*, 1459.

(3) Shvo, Y.; Czarkie, D.; Rahamin, Y.; Chodosh, D. F. *J. Am. Chem. Soc.* **1986**, *108*, 7400.

(4) (a) Menashe, N.; Shvo, Y. *Organometallics* **1991**, *10*, 3885. (b) Menashe, N.; Salant, E.; Shvo, Y. *J. Organomet. Chem.* **1996**, *514*, 97.

(5) (a) Noyori, R.; Ohkuma, T. *Pure Appl. Chem.* **1999**, *71*, 1493. (b) Ducet, H.; Ohkuma, T.; Murata, K.; Yokozama, T.; Kozawa, M.; Katayama, E.; England, A. F.; Ikariya, T.; Noyori, R. *Angew. Chem., Int. Ed.* **1998**, *37*, 1703.

10.1021/ja077525c CCC: $40.75

Scheme 2

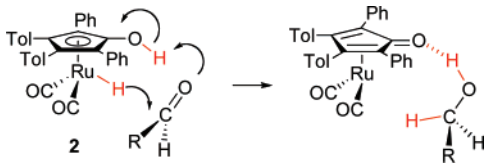

esis remains the generally accepted mechanism for the reduction of aldehydes, ketones, and imines by the Shvo catalyst.

There are two complementary ways of studying the mechanism of a catalytic process. One focuses on studies of the organometallic species thought to be involved in the process and on the kinetics and mechanisms of their reactions. Measurements of rates and activation parameters for the individual steps in a proposed catalytic mechanism can provide a kinetic model for the catalytic system. The other way of studying catalytic mechanisms involves direct observation of the catalytic system and focuses on rate of substrate conversion, the dependence of the catalytic rates on concentrations of reactants, and the nature of the organometallic species present during catalysis. When the kinetic model developed from studies of individual steps adequately accounts for the observed catalytic rates, dependencies on reactants, and nature of species present during catalysis, increased confidence can be placed in the proposed catalytic mechanism. This combination of approaches leads to a fuller understanding of the catalytic process.

For the past several years, our group has been working to elucidate the mechanism of hydrogenations catalyzed by the Shvo catalyst (**1**). Many of our studies have involved NMR measurements of complexes related to catalysis and for these studies we have used a 3,4-ditolyl variant on the Shvo catalyst that have signature tolyl methyl NMR resonances. We first examined the detailed mechanism of the reduction of aldehydes by monoruthenium hydride **2**, the active reducing agent in the Shvo catalytic cycle. We found that benzaldehyde reacted with **2** below 0 °C in a kinetically second-order process. The observation of primary kinetic isotope effects for transfer of both RuD and OD and on the failure of **2** to undergo exchange with ^{13}CO at low temperature led us to propose an outer sphere mechanism for aldehyde reduction by **2** (Scheme 2).[6−10] DFT calculations support this outer sphere mechanism and gave close estimates of the activation energy.[10a] Noyori has proposed a similar outer sphere mechanism for his ligand−metal bifunctional hydrogenation catalysts.[11] These are rare examples of reactions of transition metal complexes without prior coordination of the substrate.

Previously, we studied the loss of H_2 from ruthenium monohydride **2** as a way of gaining information about the microscopic reverse, the activation of H_2 by intermediate **A**. We reported mechanistic studies of the loss of H_2 from **2** in toluene in the presence of alcohol and of trapping PPh_3, which produces ruthenium phosphine complex **3**.[12] The rate of H_2 loss

Scheme 3. Loss of H_2 from **2** in the Presence of Alcohol

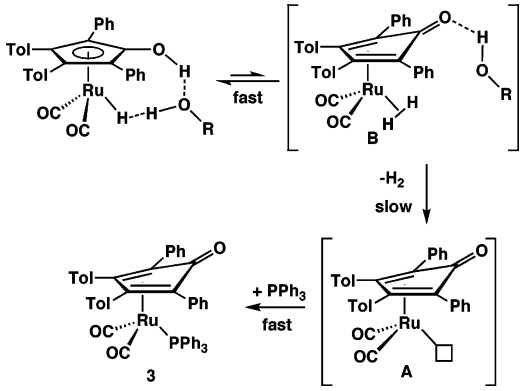

was independent of trapping [PPh_3] and was 3.7 times faster in the presence of alcohol. Exchange of label between RuD and OH was faster than loss of HD. DFT calculations supported a transition state for dihydrogen complex formation involving an ethanol bridge between the acidic CpOH and hydridic RuH of **2**; the alcohol facilitates proton transfer and accelerates the reversible formation of dihydrogen complex **B** (Scheme 3). The rate-limiting step in the presence of alcohol was proposed to be the loss of hydrogen from **B**.

To develop a full kinetic model of the hydrogenation based on rate constants for individual steps in the catalysis, we report here the determination of the rate of dissociation of diruthenium bridging hydride **1** (to **2** and **A**, k_1), and the determination of the equilibrium constant (K_{eq}) for the reaction of diruthenium bridging hydride **1** with H_2 giving two equivalents of monoruthenium hydride **2**. The ratio of the rate constants (k_2/k_{-1}) for the reactions of unsaturated intermediate **A** with H_2 and with **2** was obtained indirectly from these measurements of k_1, k_2, and K_{eq}. The kinetic model was used to simulate the rate of carbonyl compound hydrogenation and of the amounts of ruthenium species **1** and **2** present during hydrogenations.

We also report *in situ* IR spectroscopic monitoring of the catalytic hydrogenation of benzaldehyde and acetophenone with **1** ⇔ **2**. The disappearance of organic carbonyl and the concentrations of the ruthenium species present were followed throughout the hydrogenation reaction. The rate dependence on substrate, H_2 pressure, total ruthenium concentration, and solvent was measured.

The remarkable agreement found between the experimental observations of the operating catalyst system and those from kinetic model simulations provide deeper insight into the mechanism of catalysis and additional support for the basic outline of the mechanism shown in Scheme 1.

Results

Direct IR Observation of the Hydrogenation of Benzaldehyde by 1 ⇔ 2 in Toluene. The hydrogenation of benzaldehyde (0.965 M) by **1** ⇔ **2** ([**1**]$_0$ = 3.8 mM, 130:1 RCHO:Ru

(6) Casey, C. P.; Singer, S. W.; Powell, D. R.; Hayashi, R. K.; Kavana, M. *J. Am. Chem. Soc.* **2001**, *123*, 1090−1100.
(7) Casey, C. P.; Johnson, J. B. *Can. J. Chem.* **2005**, *83*, 1339.
(8) Casey, C. P.; Johnson, J. B. *J. Am. Chem. Soc.* **2005**, *127*, 1883.
(9) Bäckvall has suggested an alternative inner sphere mechanism that requires $\eta^5-\eta^3$ ring slippage. (a) Csjernyik, G.; Éll, A. H.; Fadini, L.; Pugin, B.; Bäckvall, J.-E. *J. Org. Chem.* **2002**, *67*, 1657−1662. (b) Samec, J. S. M.; Éll, A. H.; Åberg, J. B.; Privalov, T.; Eriksson, L.; Bäckvall, J.-E. *J. Am. Chem. Soc.* **2006**, *128*, 14293−14305.
(10) In the case of imine reduction, intramolecular trapping experiments support the outer sphere mechanism. (a) Casey, C. P.; Bikzhanova, G. A.; Cui, Q.; Guzei, I. A. *J. Am. Chem. Soc.* **2005**, *127*, 14062−14071. (b) Casey, C. P.; Clark, T. B.; Guzei, I. A. *J. Am. Chem. Soc.* **2007**, *129*, 11821−11827.
(11) For mechanistic and computational work on other ligand−metal bifunctional hydrogenation catalyst systems, see: (a) Yamakawa, M.; Ito, H.; Noyori, R. *J. Am. Chem. Soc.* **2000**, *122*, 1466−1478. (b) Abdur-Rashid, K.; Clapham, S. E.; Hadzovic, A.; Harvey, J. N.; Lough, A. J.; Morris, R. H. *J. Am. Chem. Soc.* **2002**, *124*, 15104−15118. (c) Sandoval, C. A.; Ohkuma, T.; Muñiz, K.; Noyori, R. *J. Am. Chem. Soc.* **2003**, *125*, 13490−13503. (d) Casey, C. P.; Johnson, J. B. *J. Org. Chem.* **2003**, *68*, 1998−2001. (e) Åberg, J. B.; Samec, J. S. M.; Bäckvall, J. -E. *Chem. Commun.* **2006**, 2771−2773.
(12) Casey, C. P.; Johnson, J. B.; Singer, S. W.; Cui, Q. *J. Am. Chem. Soc.* **2005**, *127*, 3100−3109.

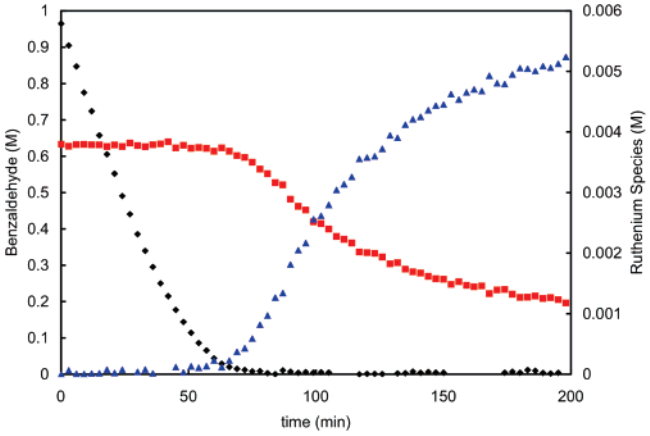

Figure 2. Concentrations of benzaldehyde (black ◆), **1** (red ■), and **2** (blue ▲) during hydrogenation of benzaldehyde (0.965 M) with 3.8 mM $[\mathbf{1}]_0$ under 35 atm hydrogen at 60 °C in toluene.

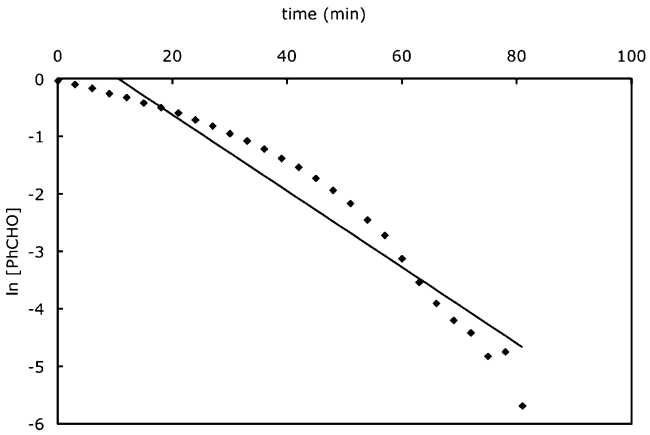

Figure 3. Plot of ln[PhCHO] vs time for hydrogenation of benzaldehyde (0.965 M) with 3.8 mM $[\mathbf{1}]_0$ under 35 atm hydrogen at 60 °C in toluene.

atom) under 35 atm hydrogen at 60 °C in toluene was monitored by *in situ* IR spectroscopy. The conversion of benzaldehyde was monitored by following the disappearance of its IR carbonyl band at 1709 cm^{-1} (Figure 2). Simultaneously, the concentrations of the ruthenium species present were monitored by following the metal carbonyl IR bands of bridging diruthenium hydride **1** at 2036, 2004, and 1997 cm^{-1} and ruthenium hydride **2** at 2018 and 1957 cm^{-1}. Quantitative measurement of **1** was made using the clean 2036 cm^{-1} band, and **2** was assumed to be the remaining material.

The disappearance of benzaldehyde did not follow a simple rate law. At low conversion, benzaldehyde conversion occurred at a nearly constant rate (approximately zero order in benzaldehyde); but at higher conversion, the rate of hydrogenation slowed. A plot of ln[PhCHO] vs time showed pronounced downward curvature (Figure 3). Clearly, the rate of conversion of benzaldehyde is not simply first order in [PhCHO]. Empirically, the hydrogenation is less than first order in benzaldehyde.

Diruthenium bridging hydride **1** was the only ruthenium species observed by IR until >90% of the benzaldehyde had been consumed (Figure 2). At equilibrium under 35 atm hydrogen, **2** is the dominant species, but **2** was not observed until after most of the benzaldehyde had been hydrogenated. Previous stoichiometric studies had shown that diruthenium complex **1** is unreactive toward benzaldehyde and that monoruthenium hydride **2** reacts rapidly with benzaldehyde even at

Table 1. Initial Rates (−d[PhCHO]/dt) for the Hydrogenation of Benzaldehyde (0.965 M) by **1** ⇔ **2** at Various Temperatures, Initial Concentrations of **1**, and Hydrogen Pressures[a]

entry	temp (°C)	$[\mathbf{1}]_0$ (mM)	H_2 (atm)	initial $-d[PhCHO]/dt \times 10^6$ M s^{-1}
1	22	5.2	35	5.70 ± 0.02
2	35	3.7	35	26.5 ± 0.2
3	35	3.8	55	37.8 ± 0.9
4	45	3.3	11	37.3 ± 0.5
5	45	3.5	11	39.9 ± 0.4
6	45	1.9	35	73 ± 3
7	45	3.9	35	79 ± 1
8	45	5.1	35	88 ± 3
9	45	3.3	55	99.9 ± 0.8
10	45	3.5	55	106 ± 1
11	60	3.8	18	245 ± 9
12	60	2.4	35	251 ± 6
13	60	3.8	35	340 ± 9

[a] Errors for rate are from linear least-squares fits. The error in the temperature is ±1 °C, which corresponds to an error of about 5% in the rate.

−40 °C.[6] Thus, **2**, the proposed active reducing agent for benzaldehyde is not present in measurable concentration during most of the hydrogenation.

The initial nearly linear portion of the concentration versus time plot (first 25% reaction, Figure 2) was used to determine initial rates of hydrogenation. These initial rates were used to determine the dependence of the rate on hydrogen pressure, total ruthenium concentration, and temperature (Table 1). The initial rate of benzaldehyde hydrogenation in toluene at 60 °C under 35 atm H_2 with $[\mathbf{1}]_0 = 3.8$ mM was (3.4×10^{-4} M s^{-1}) (Figure 2).

The rate of benzaldehyde hydrogenation increased as the total ruthenium concentration was increased, but the rate dependence was less than first order in total ruthenium. At 45 °C and 35 atm H_2, a 2.5 fold increase in the initial concentration of the bridging diruthenium hydride **1** resulted in only a 1.2 fold increase in the initial rate of hydrogenation (Table 1, entries 6−8). At 60 °C and 35 atm H_2, a 1.6 fold increase in Ru $[\mathbf{1}]_0$ led to a 1.3 fold rate increase (Table 1, entries 12−13).

The rate of benzaldehyde hydrogenation increased as the hydrogen pressure was increased, but the rate dependence on hydrogen pressure was less than first order. At 45 °C, a 5 fold increase in hydrogen pressure from 11 to 55 atm resulted in only a 2.7 fold increase in the initial rate of benzaldehyde hydrogenation when $[\mathbf{1}]_0$ was held constant at either 3.3 mM (Table 1, entries 4 and 9) or 3.5 mM (Table 1, entries 5 and 10). At 60 °C, a 2-fold pressure increase gave an initial rate increase of 1.4 (Table 1, entries 11 and 13). Similarly, at 35 °C, a pressure increase of 1.5 times from 35 to 55 atm gave an initial rate increase of 1.4 times (Table 1, entries 2 and 3).

Mechanistic and Kinetic Modeling of Benzaldehyde Hydrogenation. Any mechanistic model for the hydrogenation of benzaldehyde catalyzed by **1** ⇔ **2** faces the formidable challenge of explaining the relative concentrations of ruthenium species present during catalysis and the complex kinetics of hydrogenation, which have less than first-order dependences on aldehyde, total ruthenium, and hydrogen pressure. The mechanistic model originally proposed by Shvo (Scheme 1) involves both diruthenium bridging hydride **1** and monoruthenium hydride **2**. The steps involved include (1) the dissociation of **1** to **2** and unsaturated intermediate **A** (k_1), (2) the reduction of aldehyde by **2** which generates unsaturated intermediate **A** (k_3), (3) the

Scheme 4

$$\mathbf{1} + H_2 \underset{k_{-1}}{\overset{k_1}{\rightleftharpoons}} \mathbf{2} + \mathbf{A} + H_2 \underset{k_{-2}}{\overset{k_2}{\rightleftharpoons}} 2\,\mathbf{2}$$

$$K_{eq} = \frac{k_1 k_2}{k_{-1} k_{-2}} = \frac{[\mathbf{2}]^2}{[\mathbf{1}][H_2]} \qquad \text{Therefore,} \qquad \frac{k_2}{k_{-1}} = \frac{K_{eq} k_{-2}}{k_1}$$

loss of H_2 from **2** to generate **A** (k_{-2}), (4) reaction of **A** with H_2 to regenerate monohydride **2** (k_2), and (5) reaction **A** with **2** to regenerate **1** (k_{-1}). Knowledge of the rate constants for the first three reactions combined with the ratio of rate constants for the reactions of unsaturated intermediate **A** with H_2 and with **2** provides sufficient information to model the kinetics of benzaldehyde hydrogenation completely. If the kinetic model adequately mimics the observed complex kinetic behavior, then added confidence can be placed in the mechanistic model.

Previously, we had determined the rates and activation parameters for the stoichiometric reduction of benzaldehyde by **2** (k_3),[6,7] and for the loss of H_2 from **2** (k_{-2}).[12] Measurement of the rate of dissociation of diruthenium hydride **1** (to **2** and **A**, k_1) is detailed below. The ratio of the rate constants (k_2/k_{-1}) for the reactions of unsaturated intermediate **A** with H_2 and with **2** can be obtained by measuring the equilibrium constant for the reaction of diruthenium bridging hydride **1** with H_2 giving two equivalents of monoruthenium hydride **2** and combining it with the rates of dimer dissociation and loss of H_2 from **2** (Scheme 4).

The Rate of Dissociation of Bridging Diruthenium Hydride 1 in Toluene-d_8 was determined by monitoring the reaction of **1** with excess PPh_3 by ^1H NMR spectroscopy. The reaction proceeded cleanly at 60 °C to monoruthenium hydride **2** and Ru−PPh_3 complex **3** (Scheme 5). The kinetics of the reaction were conveniently followed at 61−82 °C in a heated NMR probe by monitoring the disappearance of **1** (δ −17.78, RuHRu) and concurrent appearance of resonances for **3** (δ 1.90, $CpTolCH_3$) and **2** (δ −9.22, RuH). Pseudo first-order rate constants were obtained from the first order nonlinear least-squares fit of the disappearance of diruthenium bridging hydride **1**. The rate of disappearance of **1** was independent of [PPh_3] (0.06−0.10 M), consistent with a unimolecular dissociation process with the rate law $-d[\mathbf{1}]/dt = k_1[\mathbf{1}]$. First-order rate constants were determined at several temperatures between 61 and 82 °C to obtain activation parameters: $\Delta H^{\ddagger} = 28.8 \pm 1.1$ kcal mol^{-1} and $\Delta S^{\ddagger} = 10.1 \pm 3.2$ eu.[13] The first-order rate constant for dissociation of **1** at 61 °C in toluene was $k_1 = 1.5 \times 10^{-4}$ s^{-1} ($t_{1/2} = 1.3$ h).

The rate of dissociation of **1** in toluene at 60 °C in the presence of PPh_3 as a trapping agent was also determined by *in situ* IR spectroscopy by following the disappearance of the IR band of **1** (2035 cm^{-1}).[13] Simultaneously, overlapping bands for **2** and **3** were observed. A first-order rate constant of $k_1 = 1.8 \pm 0.2 \times 10^{-4}$ s^{-1} ($t_{1/2} = 1.1$ h) was determined, in close agreement with measurements by NMR spectroscopy. The rate of dissociation of **1** at 60 °C was also measured in the added presence of 0.95 M benzyl alcohol using H_2 as the trapping agent ($k_1 = 3.8 \pm 0.2 \times 10^{-4}$ s^{-1}, $t_{1/2} = 0.5$ h). Benzyl alcohol sped up the dissociation of **1** by about a factor of 2.

Rate of Hydrogen Loss from Monoruthenium Hydride 2. Although loss of H_2 from **2** is too slow to be an important step in catalytic hydrogenation of carbonyl compounds, its microscopic reverse, the reaction of H_2 with the unsaturated species **A**, is a crucial step. In addition, knowledge of the rate of H_2 loss from **2** is required to obtain a quantitative estimate of the partitioning of unsaturated intermediate **A** between reaction with H_2 and reaction with **2** (k_2/k_{-1}).

Previously, we reported mechanistic studies of the loss of H_2 from **2** in toluene in the presence of trapping PPh_3, which produces ruthenium phosphine complex **3**.[12] The rate of H_2 loss was independent of trapping [PPh_3], and loss of HD was faster than exchange of label between RuD and OH in labeled **2-RuDOH**. Rate measurements between 83 °C ($t_{1/2} = 1.8$ h) and 110 °C ($t_{1/2} = 7$ min) gave $\Delta H^{\ddagger} = 26.1 \pm 1.4$ kcal mol^{-1} and $\Delta S^{\ddagger} = -3.7 \pm 3.6$ eu. Hydrogen loss from **2** at 95 °C was 3.7 times faster in the presence of alcohol and exchange of label between RuD and OH was faster than loss of HD from labeled **2-RuDOH**. DFT calculations supported a transition state for dihydrogen complex formation involving an ethanol bridge between the acidic CpOH and hydridic RuH of **2**; the alcohol facilitates proton transfer and accelerates the reversible formation of dihydrogen complex **B** (Scheme 3). The rate-limiting step in the presence of alcohol was proposed to be the loss of hydrogen from **B**.

We have estimated rate constants for H_2 loss from **2** in the presence of alcohol in toluene by multiplying the rate constant calculated from activation parameters obtained under dry conditions by 3.7, the acceleration due to alcohol measured at 95 °C. The rate estimated at 60 °C is $k_{-2} = 3.01 \times 10^{-5}$ s^{-1} ($t_{1/2} = 6.4$ h).

The Equilibrium of Bridging Diruthenium Hydride 1 and Hydrogen with Monoruthenium Hydride 2 in the Presence of Benzyl Alcohol was measured at 60 °C in toluene by *in situ* IR spectroscopy to closely match the conditions of catalytic hydrogenation (Table 1). A solution of bridging diruthenium hydride **1** and 0.95 M benzyl alcohol in toluene was heated at 60 °C under 35 atm H_2. The approach to equilibrium was monitored by observing the IR bands of **1** (2035 cm^{-1}) and **2** (2015 cm^{-1}). The equilibrium concentrations of **1** (1.8 mM) and **2** (21.3 mM), and H_2 (121 mM, calculated from measured pressures and using Henry's law and data on solubility of H_2 in toluene[14]) were used to determine an equilibrium constant of 1.9.[15]

Scheme 5. Reaction of **1** with PPh_3 or H_2 Trapping

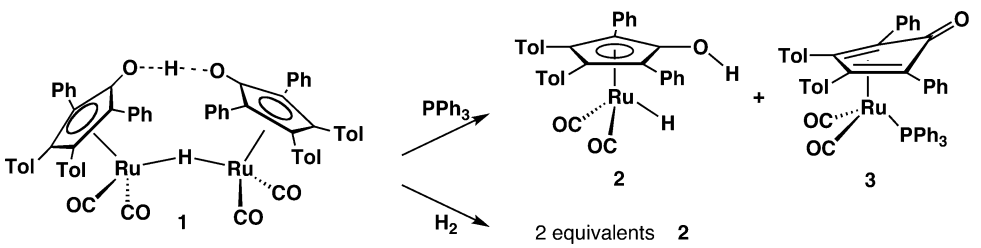

Table 2. Rate and Equilibrium Constants Used to Model the Hydrogenation of Benzaldehyde and Acetophenone by **1** ⇔ **2** in Toluene at 60 °C under 35 atm Hydrogen

k_1	$3.80 \times 10^{-4}\ s^{-1}$	Measured at 60 °C in presence of benzyl alcohol
k_{-2}		$\Delta H^{\ddagger} = 26.1$ kcal mol^{-1}
	$3.01 \times 10^{-5}\ s^{-1}$	$\Delta S^{\ddagger} = -3.7$ eu Rates measured between 83 and 110 °C Corrected for 3.7-fold acceleration by alcohol
K_{eq}	1.9	Measured at 60 °C in presence of benzyl alcohol
k_2/k_{-1}	0.15	$k_2/k_{-1} = K_{eq}(k_{-2}/k_1)$
k_3 PhCHO	$40\ M^{-1}s^{-1}$	$\Delta H^{\ddagger} = 13.0$ kcal mol^{-1} $\Delta S^{\ddagger} = -12.4$ eu. Rates measured between −26 and −49 °C in absence of added alcohol
k_3 PhCOMe	$0.43\ M^{-1}s^{-1}$	$\Delta H^{\ddagger} = 12.6$ kcal mol^{-1} $\Delta S^{\ddagger} = -22.6$ eu. Rates measured between −6 and 17 °C in absence of added alcohol

The equilibrium was also measured by ^{1}H NMR spectroscopy at much lower pressure. Toluene-d_8 solutions of bridging diruthenium hydride **1** (5.89 mM) under 3.7 atm of H_2 in the presence of 34 mM benzyl alcohol were heated at 60 °C for two weeks, and the concentrations of **1** (δ −17.78, RuHRu, 2.5 mM), **2** (δ −9.36, RuH, 7.0 mM), and H_2 (δ 4.51, 13 mM)[16] were determined by ^{1}H NMR integration. An equilibrium constant of 1.5 was determined. A similar value was obtained in the absence of benzyl alcohol.

Partitioning of Unsaturated Intermediate A between Reaction with H_2 and with Ruthenium Hydride 2. The partitioning ratios for reaction of intermediate **A** with H_2 (k_2) and with **2** (k_{-1}) in toluene containing benzyl alcohol were calculated at 60 °C from the rate of dissociation of **1** ($k_1 = 3.8 \times 10^{-4}\ s^{-1}$), the rate of H_2 loss from **2** ($k_{-2} = 3.01 \times 10^{-5}\ s^{-1}$), and the equilibrium constant ($K_{eq} = 1.9$) as shown in the equation in Scheme 4. Whereas k_1 and K_{eq} were measured directly at 60 °C in the presence of benzyl alcohol, k_{-2} was calculated from activation parameters determined in the absence of alcohol and corrected for 3.7 fold acceleration in the presence of alcohol. At 60 °C, $k_2/k_{-1} = 0.15$. The partitioning of the intermediate depends on the concentrations of H_2 and ruthenium monohydride **2** ($k_2[H_2]/k_{-1}[\mathbf{2}]$). Because the concentration of **2** was immeasurably low until most of the benzaldehyde was hydrogenated, the majority of intermediate **A** is predicted to react with H_2 to regenerate **2** during catalysis.

Rate of Reduction of Benzaldehyde by 2 in Toluene-d_8. The rate of benzaldehyde reduction by **2** in toluene-d_8 has been previously reported; rates measured between −26 and −49 °C gave activation parameters of $\Delta H^{\ddagger} = 13.0 \pm 1.8$ kcal mol^{-1} and $\Delta S^{\ddagger} = -12.4 \pm 5.1$ eu.[6,7,17] The rate constant calculated at 60 °C is 81.0 $M^{-1}s^{-1}$.

Kinetic Modeling of the Hydrogenation of Benzaldehyde with 1 ⇔ 2 in Toluene. With estimates of all the needed rate constants in hand (Table 2), we modeled the kinetics of the catalytic hydrogenation [35 atm H_2 = 140 mM] of benzaldehyde [0.97 M] with **1** ⇔ **2** ([**1**]$_0$ = 3.8 mM) in toluene at 60 °C according to the mechanism shown in Scheme 1 using KinTekSim modeling software.[18] Because hydrogen pressure and thus hydrogen concentration were constant, the reaction of **A** with hydrogen was expressed as a unimolecular reaction of **A** going to **2** with the rate = $k[\mathbf{A}] = k_2[H_2][\mathbf{A}]$. The rate constants for reaction of reactive intermediate **A** with H_2 and with **2** were given arbitrarily large values ($k_{-1} = 10^5\ s^{-1}$, $k_2[H_2] = 2.2 \times 10^3\ s^{-1}$) with the ratio of k_2/k_{-1} set at 0.15. Large values of k_2 and k_{-1} are required to avoid build-up of the unseen reactive intermediate **A** in the simulation.

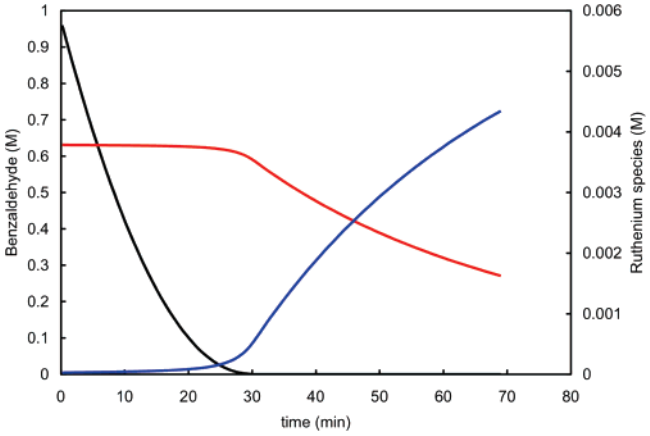

Figure 4. Kinetic modeling simulations of concentrations of benzaldehyde (black), **1** (red), and **2** (blue) during hydrogenation of benzaldehyde (0.965 M) with 3.8 mM [**1**]$_0$ under 35 atm hydrogen at 60 °C in toluene. (See Figure 2 for comparison with experimental line shapes, note difference of time scales).

This kinetic simulation was used to calculate the time course of the concentrations of benzaldehyde and the ruthenium species **1** and **2** (Figure 4). This simulation should be compared with the experimentally observed course of benzaldehyde hydrogenation (Figure 2). The first thing to notice is the similarity of the shape of the curves for benzaldehyde disappearance. Both the simulated and experimental rates show an initial nearly linear portion with rates slowing as a function of benzaldehyde conversion. For example, compared to the initial rate (−d[PhCHO]/dt), the rate at 50% conversion is 9% slower experimentally and 20% slower in the model, and the rate at 90% conversion is 50% slower experimentally and 59% slower in the model.

The kinetic simulation correctly mirrors the concentrations of the ruthenium species present during hydrogenation of benzaldehyde. Experimentally, only diruthenium bridging hydride **1** is seen until ≥95% conversion of benzaldehyde; in the model, **1** constitutes 99% of total ruthenium at 95% conversion.

The simulation predicts a 3.0 fold faster initial rate (1.04×10^{-3} M s^{-1}) of hydrogenation of benzaldehyde than experimentally observed. This is remarkably good considering that the simulation relied on activation parameters to extrapolate rate constants to 60 °C from either much lower or much higher temperatures. In particular, the major uncertainty in the rate constants comes from the extrapolation of k_3, the rate constant for reaction of **2** with RCH═O, to 60 °C using activation parameters determined at 100 °C lower temperature.[19]

(13) See Tables S1 and S3 and Figure S1 in Supporting Information for rate constants and Eyring plot.
(14) Brunner, E. *J. Chem. Eng. Data* **1985**, *30*, 269.
(15) See Table S5 in Supporting Information.
(16) The concentration of H_2 in solution was corrected for under-integration due to para hydrogen by multiplying the integral by 4/3. Bonhoeffer, K. F.; Harteck, P. *Z. Phys. Chem. B* **1929**, *4*, 113.
(17) The rates and activation parameters reported here are for disappearance of carbonyl compound. The rates are one-half of the previously reported rates of disappearance of RuH **2**.[7] Because each reduction of carbonyl compound leads to the consumption of 2 equiv of **2**, the rate constant for the reduction of carbonyl compound is 1/2 that for disappearance of **2**.
(18) Program available from Kin Tek Corporation. Barshop, B. A.; Wrenn, R. F.; Frieden, C. *Analytical Biochem.* **1983**, *130*, 134.

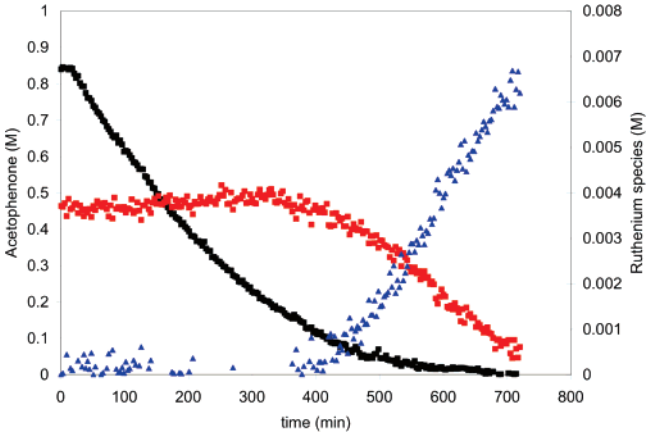

Figure 5. Concentrations of acetophenone (black ◆), **1** (red ■), and **2** (blue ▲) during hydrogenation of acetophenone (0.84 M) with 3.7 mM $[\mathbf{1}]_0$ under 35 atm hydrogen at 60 °C in toluene.

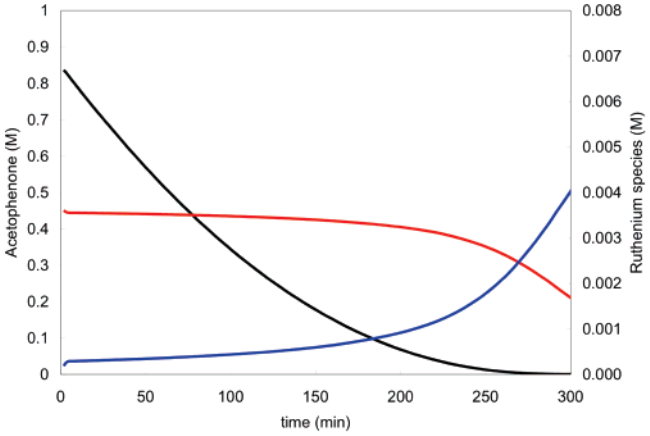

Figure 6. Kinetic modeling simulations of **c**oncentrations of acetophenone (black), **1** (red), and **2** (blue) during hydrogenation of acetophenone (0.84 M) with 3.7 mM $[\mathbf{1}]_0$ under 35 atm hydrogen at 60 °C in toluene. (See Figure 5 for comparison with experimental line shapes, note difference of time scales).

The kinetic simulation model adequately accounts for the less than first-order dependences of the initial rates of benzaldehyde hydrogenation on total ruthenium and on H_2 pressure. A simulation with 1.6 times the amount of catalyst ($[\mathbf{1}]_0 = 3.8$ mM compared to 2.4 mM) increased the initial rate of benzaldehyde conversion by a factor of 1.29.[20] Experimentally, increasing $[\mathbf{1}]_0$ by a factor of 1.6 gave a 1.35-fold increase in the initial rate (Table 1, entries 12 and 13). In simulations, increasing pressure from 18 to 35 atm H_2 gave a 1.45-fold increase in the initial hydrogenation rate. Experimentally, increasing pressure from 18 to 35 atm H_2 gave a 1.42-fold increase (Table 1, entries 11 and 13). In related experiments at 45 °C, a 5-fold increase in H_2 pressure resulted in a 2.7-fold rate increase (Table 1, entries 4, 5, 7, 9, and 10).

Comparison of the Rate of Benzaldehyde Hydrogenation with the Rate of Dissociation of Bridging Ruthenium Hydride 1 provides additional insight into the mechanism of hydrogenation. The rate constant for dissociation of **1** at 60 °C in toluene ($k_1 = 3.8 \times 10^{-4}$ s^{-1}) taken together with $[\mathbf{1}]_0 = 3.8$ mM gives a rate of dissociation of 1.44×10^{-6} M s^{-1}. Since almost all of the reactive intermediate **A** generated by dissociation of **1** reacts with H_2 to give an additional equivalent of **2**,[21] the rate of formation of **2** (2.89×10^{-6} M s^{-1}) is twice the rate of disappearance of **1**. The initial rate of benzaldehyde hydrogenation in toluene at 60 °C under 35 atm H_2 (3.4×10^{-4} M s^{-1}) was 120 times larger than the rate of generation of **2** from **1**. This indicates that every dissociation of **1** to the ruthenium monohydride active reducing agent **2** and unsaturated intermediate **A** is responsible for 240 cycles of benzaldehyde hydrogenation (Scheme 1). After 95% hydrogenation of benzaldehyde, the instantaneous rate had dropped to 1.02×10^{-4} M s^{-1}; at this point the concentration of **1** has dropped slightly to 3.7 mM, which gives a rate of dissociation of **1** of 1.4×10^{-6} M s^{-1}. At this point, only 72 benzaldehyde hydrogenation cycles are occurring for each dissociation of **1**.

In the kinetic simulation model during the first 25% conversion, every dissociation of **1** results in 720 cycles of benzaldehyde hydrogenation.

Estimation of the Concentration of Monoruthenium Hydride 2 During Hydrogenation was made using the mechanistic model in which **2** is the active reducing agent (Scheme 1). In terms of this mechanism, the measured initial rate of benzaldehyde hydrogenation is equal to the rate of reaction of benzaldehyde with the small amount of **2** present ($-$d[PhCHO]/dt $= k_3[\mathbf{2}]$[PhCHO]). Extrapolation of k_3 to 60 °C from measurements made at between -26 and -49 °C, using $\Delta H^{\ddagger} = 13.0 \pm$ kcal mol^{-1} and $\Delta S^{\ddagger} = -12.4 \pm$ eu, gave $k_3 = 40$ M^{-1}s^{-1}. Using the early [PhCHO] = 0.84 M (midpoint of initial rate measurement), and the observed initial rate of benzaldehyde hydrogenation ($-$d[PhCHO]/dt $= 3.4 \times 10^{-4}$ M s^{-1}) leads to an estimate of [**2**] = 0.009 mM, which is less than 0.2% of the ruthenium atoms.[22] This is consistent with the failure to observe **2** by *in situ* IR spectroscopy during the first 25% conversion of benzaldehyde.

Estimation the Partitioning Ratio for Reaction of A with H_2 and with Ruthenium Hydride 2. As pointed out above, every dissociation of **1** effectively produces 2 equiv of **2** and results in hydrogenation of 240 equiv of benzaldehyde. This means that every time reactive intermediate **A** is generated from reduction of benzaldehyde by **2**, it reacts with H_2 to regenerate **2** 240 times faster than it reacts with **2** to form **1**. Using the estimated concentration of [**2**] = 0.009 mM along with the $[H_2]$ = 0.146 M at 35 atm, the partitioning ratio k_2/k_{-1} is calculated as 0.015. This a factor of 10 less than that used in the simulations.[23]

$$\frac{k_2[H_2]}{k_{-1}[\mathbf{2}]} = 240\,\frac{k_2}{k_{-1}} = \frac{240 \times (9 \times 10^{-6})}{0.146} = 0.015$$

(19) The simulations provide a very close fit to the experimental initial rate of hydrogenation of benzaldehyde if a 3.0 fold smaller value of $k_3 = 13.3$ M^{-1}s^{-1} is employed; this value is well within the error range of k_3 values (2.6 to 600 M^{-1}s^{-1} based on the error limits for the activation parameters).
(20) See Table S11 in Supporting Information for details of these simulations.
(21) Under catalytic conditions, reactive intermediate **A** reacts with H_2 much faster than it combines with **2** to regenerate the unreactive diruthenium bridging hydride **1**. This is due in part to the very low concentration of **2** present during benzaldehyde hydrogenation.
(22) In an earlier footnote,[19] we pointed out that if a 3.0-fold lower value of k_3 were used then a better match to overall rate was obtained. Using this lower value of k_3, then [**2**] is calculated to be 2.5 times greater or 0.022 mM (0.3% of total Ru).
(23) If a higher concentration of [**2**] = 0.022 mM were used (related to a possible underestimate of k_3), then the partitioning ratio k_2/k_{-1} is calculated as 0.036, in somewhat closer agreement with the value of 0.15, which was calculated from K_{eq}, k_1, and k_{-2} and used in the simulations.

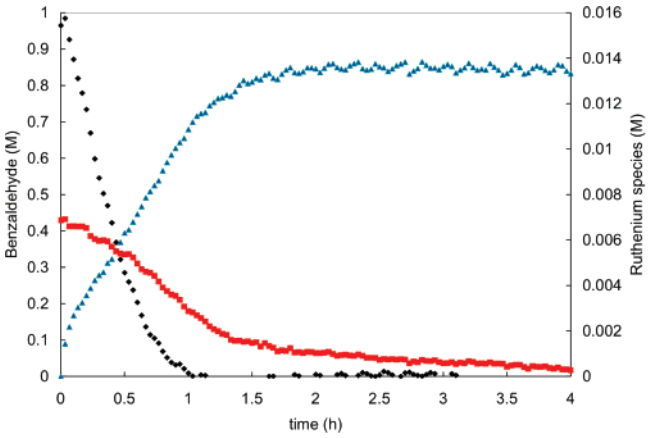

Figure 7. Concentrations of benzaldehyde (black ◆), **1** (red ■), and **2** (blue ▲) during hydrogenation of benzaldehyde (0.965 M) with 6.9 mM $[\mathbf{1}]_0$ under 35 atm H_2 at 60 °C in THF.

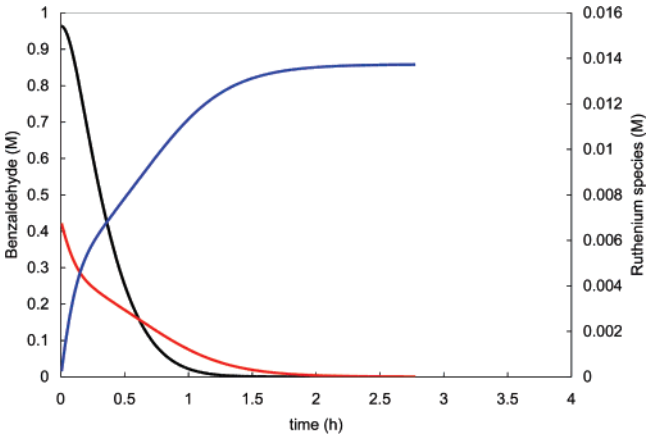

Figure 8. Kinetic modeling simulations of concentrations of benzaldehyde (black), **1** (red), and **2** (blue) during hydrogenation of benzaldehyde (0.97 M) with 6.9 mM $[\mathbf{1}]_0$ under 35 atm hydrogen at 60 °C in THF. (Same scale as experimental data Figure 7).

The Observed Concentration of 2 During Hydrogenation is Far Below its Equilibrium Value because it is driven down by very rapid reaction with benzaldehyde. Whereas **A** is converted to monohydride **2** 240 times faster than it reacts with **2** to produce inactive **1**, reaction of **2** with benzaldehyde continually regenerates **A** and eventually **A** and **2** react with each other to form **1**. In other words, the rapid reaction of **2** with benzaldehyde drives down the concentration of **2** and prevents it from approaching its equilibrium value until after the benzaldehyde is consumed.

Direct IR Observation of the Hydrogenation of Acetophenone by 1 ⇔ 2 in Toluene. The hydrogenation of acetophenone (0.84 M) by **1** ⇔ **2** ($[\mathbf{1}]_0$ = 3.7 mM, 130:1 PhCOMe:Ru atom) under 35 atm hydrogen in toluene at 60 °C was monitored by *in situ* IR spectroscopy. The conversion of acetophenone was monitored by following the disappearance of its IR carbonyl band at 1690 cm^{-1} (Figure 5). Simultaneously, **1** (2036, 2004, and 1997 cm^{-1}) and **2** (2018 and 1957 cm^{-1}) were followed. Quantitative measurement of **1** was made using the clean 2036 cm^{-1} band, and **2** was assumed to be the remaining material. Low concentrations of **2** were seen during acetophenone hydrogenation, and significant amounts of **2** were seen only after most of the acetophenone had been hydrogenated.

After a short initial induction period, the initial rate of conversion of acetophenone (−d[PhCOMe]/dt) was 4.82×10^{-5} M s^{-1}, which was about 7 times slower than the initial rate of hydrogenation of benzaldehyde under similar conditions. For comparison, when a mixture of benzaldehyde and acetophenone was hydrogenated, acetophenone was hydrogenated 40 times slower than benzaldehyde.[24] The stoichiometric rate of reduction of acetophenone by **2** at 60 °C (estimated from activation parameters) was 90 times slower than that of benzaldehyde.

Kinetic Modeling of the Hydrogenation of Acetophenone with 1 ⇔ 2 in Toluene. The same rate constants were used as for benzaldehyde modeling except for k_3, the rate constant for reduction of acetophenone by **2** in toluene-d_8. Activation parameters ($\Delta H^{\ddagger} = 12.6 \pm 1.10$ kcal mol^{-1} and $\Delta S^{\ddagger} = -22.6 \pm 2.8$ eu determined from rates measured between −6 °C and 17 °C)[17] were used to calculate $k_3 = 0.43$ $M^{-1}s^{-1}$. The initial simulated rate of hydrogenation of acetophenone (9.7×10^{-5} M s^{-1}) was two times faster than the experimental rate (Figure 6). Considering the different temperatures used in measuring the rate constants used in the simulations, the agreement between the simulation and experimental results is even better than anticipated. The simulation showed that about 4.4% of the ruthenium was present as **2** at 25% conversion of acetophenone; this is in qualitative agreement with experiment.

The experimental initial rate of acetophenone hydrogenation (4.82×10^{-5} M s^{-1}) was 34 times faster than the calculated rate of dissociation of bridging ruthenium hydride **1** (1.4×10^{-6} M s^{-1})[25] and 17 times faster than generation of **2** from **1**. This indicates that every dissociation of **1** to active reducing agent **2** and unsaturated intermediate **A** is responsible for 34 cycles of acetophenone hydrogenation (Scheme 1). This is fewer cycles than the 240 cycles for benzaldehyde.

An estimation of [**2**] present during acetophenone hydrogenation at 25% conversion was made using $-d[PhCOMe]/dt = k_3[\mathbf{2}][PhCOMe]$, which gave [**2**] = 0.17 mM (2.2% of Ru). This is consistent with the small but measurable concentration of **2** observed during catalysis. It is also in agreement with the simulation's calculation of 4.4% of Ru present as **2**.

Direct IR Observation of the Hydrogenation of Benzaldehyde by 1 ⇔ 2 in Tetrahydrofuran. Although toluene is our preferred solvent for hydrogenations, many of the initial studies of the stoichiometric reduction of aldehydes with monoruthenium hydride **2** were performed in tetrahydrofuran. To gain understanding on how the choice of solvent affects hydrogenation with **1** ⇔ **2**, we also examined and modeled the hydrogenation of benzaldehyde and acetophenone in THF.

The hydrogenation of benzaldehyde (0.97 M) by **1** ⇔ **2** ($[\mathbf{1}]_0$ = 6.9 mM, 70:1 PhCHO:Ru atom) under 35 atm H_2 in THF at 60 °C was monitored by *in situ* IR spectroscopy. The conversion of benzaldehyde was monitored by following the disappearance of its IR carbonyl band at 1706 cm^{-1} (Figure 7). Simultaneously, **1** (2036, 2004, and 1997 cm^{-1}) and **2** (2018 and 1957 cm^{-1}) were followed. Quantitative measurement of **1** was made using the clean 2036 cm^{-1} band, and **2** was assumed to be the remaining material. In contrast to observations in toluene,

(24) Casey, C. P.; Strotman, N. A.; Beetner, S. E.; Johnson, J. B.; Priebe, D. C.; Guzei, I. A. *Organometallics* **2006**, *25*, 1236−1244.

(25) Rate of dissociation of **1** at 60 °C in toluene is given by $k_1[\mathbf{1}]_0 = 3.8 \times 10^{-4}$ $s^{-1} \times$ [3.7 mM].

substantial and growing concentrations of **2** were seen throughout the hydrogenation of benzaldehyde in THF.

The initial rate of hydrogenation of benzaldehyde in THF was 3.6×10^{-4} M s^{-1} using 6.9 mM $[\mathbf{1}]_0$. This is about the same rate as seen in toluene using about half the amount of catalyst ($[\mathbf{1}]_0 = 3.8$ mM). The stoichiometric rate of reduction of benzaldehyde by **2** in THF at 60 °C was estimated to be 560 times slower than that of benzaldehyde in toluene using activation parameters.

Parameters for Kinetic Modeling of Hydrogenations in THF were obtained in a similar manner to that employed for modeling in toluene. Published data provided the rates and activation parameters for the stoichiometric reduction of benzaldehyde and of acetophenone by **2** (k_3) in THF.[6,7] New measurements of the rate of dissociation of **1** (k_1), the equilibrium constant for the conversion of **1** and H_2 to **2**, and the rate of H_2 loss from **2** (k_{-2}) in THF were needed for the model.

The Rate of Dissociation of Bridging Diruthenium Hydride 1 in THF-d_8 was determined by monitoring the reaction of **1** with excess PPh_3 (0.050−0.085 M) by ^{1}H NMR spectroscopy. The disappearance of **1** followed the same rate law as in toluene, $-d[\mathbf{1}]/dt = k_1[\mathbf{1}]$ and was independent of $[PPh_3]$. First-order rate constants determined between 45 and 63 °C gave activation parameters: $\Delta H^{\ddagger} = 21.6 \pm 0.6$ kcal·mol^{-1} and $\Delta S^{\ddagger} = -6.7 \pm 2.1$ eu ($k_1 = 1.62 \times 10^{-3}$ s^{-1} at 60 °C).[26] The dissociation of **1** in THF was also monitored by IR at 60 °C using PPh_3 as the trapping agent.[26] The rate measured by IR ($k_1 = 1.51 \times 10^{-3}$ s^{-1}) was in close agreement with the NMR measurements and was used in simulations. The rate of dissociation of **1** is about four times faster in THF than in toluene.

The Equilibrium Between Bridging Diruthenium Hydride 1 plus H_2 and Monoruthenium Hydride 2 in THF was measured by ^{1}H NMR spectroscopy. Since the equilibrium lies much farther to the side of **2** in THF than in toluene, much lower pressures of H_2 were used. THF-d_8 solutions of **1** (19.6 mM) containing $PhCH_2OH$ (0.64 M)[27] in two resealable NMR tubes were pressurized with H_2 (200 Torr at 77 K, 0.26 atm) and allowed to equilibrate at 60 °C over 8 days. In the two tubes, concentrations of **1** (δ −18.26, 2.9, and 1.2 mM), **2** (δ −9.75, 33 and 37 mM), and H_2 (δ 4.75, 15 and 19 mM)[16] were determined by integration of ^{1}H NMR spectra; $K_{eq} = 25$ and 62 at 60 °C. The average of these two equilibrium constants $K_{eq} = 43$ was used in simulations. IR observation of equilibrium mixtures of **1** and **2** under 35 atm H_2 at 60 °C showed only **2** in agreement with the equilibrium constants determined at much lower pressure.

Hydrogen Loss from Ruthenium Hydride 2 in THF-d_8, occurred about 22 times slower than in dry toluene-d_8. When THF-d_8 solutions of **2** (0.015−0.025 M) containing excess PPh_3 were heated at 95 °C and monitored by ^{1}H NMR spectroscopy, clean conversion to phosphine complex **3** was observed. The disappearance of **2** followed first-order kinetics and the observed rate constant was independent of $[PPh_3]$ (0.20−0.40 M), consistent with the rate law: $-d[\mathbf{2}]/dt = k_2[\mathbf{2}]$. The rate was measured between 86 and 101 °C for the determination of activation parameters: $\Delta H^{\ddagger} = 31.7 \pm 0.8$ kcal mol^{-1} and $\Delta S^{\ddagger} = 9.8 \pm 2.2$ eu.[28] The rate extrapolated to 60 °C was 1.54×10^{-6} s^{-1}, $t_{1/2} = 125$ h.

The rate of H_2 loss from **2** in THF using CO as a trapping agent was measured in the presence of 0.9 M benzyl alcohol at 60 °C in a ReactIR apparatus. The disappearance of **2** (2015 cm^{-1}) and appearance of ruthenium tricarbonyl complex [2,5-Ph_2-3,4-Tol_2(h^4-$C_4C{=}O$)]$Ru(CO)_3$ (2080 cm^{-1}) were followed. The measured rate ($k_{-2} = 3.09 \times 10^{-6}$ s^{-1}, $t_{1/2} = 62$ h) was similar to that estimated above and was used in the simulations.

Partitioning Ratio for Unsaturated Intermediate A between Reaction with H_2 and with Ruthenium Hydride 2 in THF was calculated at 60 °C from k_1, k_{-2}, and K_{eq} all measured at 60 °C (Scheme 4). The calculated ratio in THF was $k_2/k_{-1} = 9.28$ which is 110 times larger than in toluene. The difference is due both to the much larger equilibrium constant in THF and to faster rate of dissociation of **1** in THF. Taken alone, this rate constant ratio favors reaction of **A** with H_2 over **2** in THF compared with toluene. However, the greater rate of dissociation of **1** and the slower rate of reaction of aldehyde with **2** leads to a much greater concentration of **2** during hydrogenations in THF compared with toluene. These effects operate in opposite directions for the partitioning of **A**.

Rates of Reduction of Benzaldehyde and of Acetophenone by 2 in THF have been previously reported. Rates of benzaldehyde reduction by **2** in THF-d_8 were measured between 10 and 34 °C to give activation parameters: $\Delta H^{\ddagger} = 13.4 \pm 0.9$ kcal mol^{-1} and $\Delta S^{\ddagger} = -22.9 \pm 2.6$ eu.[17] The rate constant calculated at 60 °C is 7.1×10^{-2} $M^{-1}s^{-1}$was used in simulations.

Rates of acetophenone reduction by **2** in THF-d_8 were measured between 51 and 73 °C to give activation parameters: $\Delta H^{\ddagger} = 17.5 \pm 1.2$ kcal mol^{-1} and $\Delta S^{\ddagger} = -17.3 \pm 4.0$ eu.[17] The rate constant calculated at 60 °C is 8.08×10^{-3} $M^{-1}s^{-1}$was used in simulations.

Kinetic Modeling of the Hydrogenation of Benzaldehyde with 1 ⇔ 2 in THF employed the rate constants shown in Table 3, $[H_2] = 140$ mM (35 atm), initial benzaldehyde [0.97 M], $[\mathbf{1}]_0 = 6.9$ mM. As in the case of simulation in toluene, the reaction of **A** with H_2 was expressed as a unimolecular reaction of **A** going to **2** with the rate $= k[\mathbf{A}] = k_2[H_2][\mathbf{A}]$, and the rate constants for reaction of reactive intermediate **A** with H_2 and with **2** were given arbitrarily large values ($k_{-1} = 10^5$ s^{-1}, $k_2[H_2] = 1.3 \times 10^4$ s^{-1}) with the ratio of k_2/k_{-1} set at 9.28.

The simulation obtained using KinTekSim modeling software[18] shows that the initial rate of benzaldehyde hydrogenation (4.4×10^{-4} M s^{-1}) is very close to the experimental initial rate (3.6×10^{-4} M s^{-1}) (Figure 8). The simulation shows significant concentrations of ruthenium monohydride **2** during the hydrogenation of benzaldehyde. For example, after 50% conversion of benzaldehyde, the simulation shows $[\mathbf{2}] = 6.5$ mM (47% of Ru) compared with the experimental observation of $[\mathbf{2}] = 5.0$ mM (30% of Ru).[29] The simulation of the rise of $[\mathbf{2}]$ shows the same unusual shape as seen in the experimental observations. The slower rate of reaction of benzaldehyde with

(26) See Tables S2 and S4 and Figure S2 in Supporting Information for rates and Eyring plot.
(27) The initial concentration of $PhCH_2OH$ was reduced slightly by dehydrogenation of benzyl alcohol followed by a ruthenium catalyzed Tischenko disproportionation to give some benzyl benzoate. The dehydrogenation increased the amount of H_2 present in solution.
(28) See Table S6 and Figure S3 in Supporting Information for rate constants and Eyring plot.
(29) After 25% conversion of benzaldehyde, the simulation shows $[\mathbf{2}] = 5.1$ mM (37% of Ru) compared with the experimental observation of $[\mathbf{2}] = 3.6$ mM (21% of Ru).

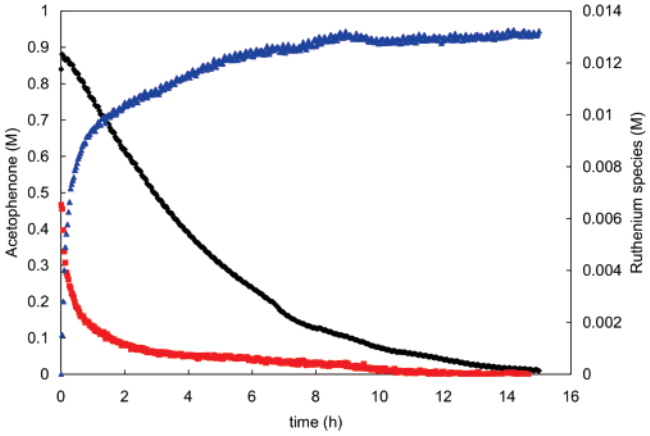

Figure 9. Concentrations of acetophenone (black ◆), **1** (red ■), and **2** (blue ▲) during hydrogenation of acetophenone (0.84 M) in THF with 6.5 mM $[\mathbf{1}]_0$ at 60 °C under 35 atm H_2.

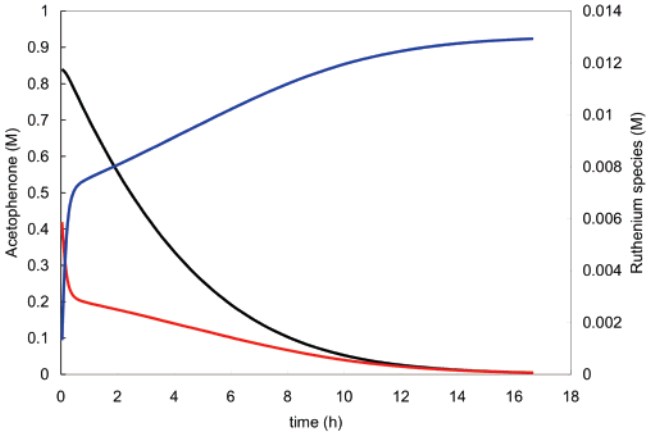

Figure 10. Kinetic modeling simulations of concentrations of acetophenone (black), **1** (red), and **2** (blue) during hydrogenation of acetophenone (0.84 M) in THF with 6.5 mM $[\mathbf{1}]_0$ at 60 °C under 35 atm H_2. (Same scale as experimental data Figure 9.)

2 in THF than in toluene allows the build up of significant concentrations of **2**.

The experimental initial rate of benzaldehyde hydrogenation (3.6×10^{-4} M s^{-1}) was 36 times faster than the calculated rate of dissociation of bridging ruthenium hydride **1** (9.8×10^{-6} M s^{-1})[30] and 18 times faster than generation of **2** from **1**. This indicates that every dissociation of **1** to active reducing agent **2** and unsaturated intermediate **A** is responsible for 36 cycles of benzaldehyde hydrogenation (Scheme 1). This is fewer cycles than the 240 cycles for benzaldehyde hydrogenation in toluene.

The initial rate of benzaldehyde hydrogenation in THF can be predicted from direct measurement of [**2**] = 5.0 mM at 25% benzaldehyde hydrogenation and from the rate constant for stoichiometric reduction of benzaldehyde by **2** calculated from activation parameters determined at lower temperature: $-$d[PhCHO]/dt = k_3[**2**][PhCHO] = 7.10×10^{-2} $M^{-1}s^{-1}$ [5.0×10^{-3} M][0.84 M] = 2.9×10^{-4} $M^{-1}s^{-1}$. This estimate is in remarkably close agreement with the experimentally observed initial rate of benzaldehyde hydrogenation (3.6×10^{-4} M s^{-1}).

Direct IR Observation of the Hydrogenation of Acetophenone by 1 ⇔ 2 in THF. The hydrogenation of acetophenone (0.84 M) by **1** ⇔ **2** ($[\mathbf{1}]_0$ = 6.5 mM, 70:1 PhCOMe:Ru atom) under 35 atm H_2 in THF at 60 °C was monitored by *in situ* IR spectroscopy. The conversion of acetophenone was monitored by following the disappearance of its IR carbonyl band at 1690 cm^{-1} (Figure 9). Simultaneously, **1** (2036, 2004, and 1997 cm^{-1}) and **2** (2018 and 1957 cm^{-1}) were followed. Quantitative measurement of **1** was made using the clean 2036 cm^{-1} band, and **2** was assumed to be the remaining material. The concentration of **2** rose rapidly and was relatively high throughout the hydrogenation. For example, at 50% conversion of acetophenone, monoruthenium hydride **2** constituted 88% of the ruthenium present.

The initial rate of hydrogenation of acetophenone in THF was $3.9 \pm 0.2 \times 10^{-5}$ M s^{-1} using 6.5 mM $[\mathbf{1}]_0$ which was slightly slower than the rate in toluene (4.82×10^{-5} M s^{-1}) using about half the amount of catalyst ($[\mathbf{1}]_0$ = 3.7 mM). The stoichiometric rate of reduction of acetophenone by **2** in THF at 60 °C was estimated to be 115 times slower than that of acetophenone in toluene using activation parameters.

Table 3. Rate and Equilibrium Constants Used to Model the Hydrogenation of Benzaldehyde and Acetophenone by **1** ⇔ **2** in THF at 60 °C under 35 atm H_2

k_1	1.51×10^{-3} s^{-1}	IR rate measured at 60 °C in absence of alcohol
k_{-2}	3.09×10^{-6} s^{-1}	$\Delta H^{\ddagger} = 31.7$ kcal mol^{-1} $\Delta S^{\ddagger} = 9.8$ eu. Rates measured by NMR between 86 and 101 °C. Rate used was determined by IR at 60 °C
k_2/k_{-1}	9.28	$k_2/k_{-1} = K_{eq}$ (k_{-2}/k_1)
K_{eq}	43	Measured by NMR at 60 °C in presence of benzyl alcohol
k_3 PhCHO	7.10×10^{-2} M^{-1} s^{-1}	$\Delta H^{\ddagger} = 13.4 \pm 0.9$ kcal mol^{-1} $\Delta S^{\ddagger} = -22.9 \pm 2.6$ eu. Rates measured between 10 and 34 °C in absence of added alcohol
k_3 PhCOMe	8.08×10^{-3} M^{-1} s^{-1}	$\Delta H^{\ddagger} = 17.5 \pm 1.2$ kcal mol^{-1} $\Delta S^{\ddagger} = -17.3 \pm 4.0$ eu. Rates measured between 51 and 73 °C in absence of added alcohol

The initial rate hydrogenation of acetophenone in THF was about 9 times slower than that of benzaldehyde under similar conditions. The stoichiometric rate of reduction of acetophenone by **2** at 60 °C in THF (estimated from activation parameters) was 30 times slower than that of benzaldehyde.

Kinetic Modeling of the Hydrogenation of Acetophenone with 1 ⇔ 2 in THF. The same rate constants were used as for benzaldehyde modeling except for k_3, the rate constant for reduction of acetophenone by **2** in THF. The initial simulated rate of hydrogenation of acetophenone (4.5×10^{-5} M s^{-1}) was only 15% faster than the experimental rate. The simulation showed 66% of the ruthenium was present as **2** at 50% conversion of acetophenone; this is in qualitative agreement with experiment (Figure 10).

The experimental initial rate of acetophenone hydrogenation in THF ($3.9 \pm 0.2 \times 10^{-5}$ M s^{-1}) was only about twice as fast as the calculated rate of dissociation of bridging ruthenium hydride **1** (1.72×10^{-5} M s^{-1})[31] and about the same as the rate of generation of **2** from **1**. This indicates that the rate of hydrogenation of acetophenone in THF is not severely limited

(30) The rate of dissociation of **1** at 60 °C in THF is given by $k_1[\mathbf{1}]_{50\%} = 1.51 \times 10^{-3}$ s^{-1} × [6.5 mM].

(31) The rate of dissociation of **1** at 60 °C in THF is given by $k_1[\mathbf{1}]_{50\%} = 1.51 \times 10^{-3}$ s^{-1} × [11.4 mM].

Table 4. Comparison of Experimental and Simulated Rates of Hydrogenation of Benzaldehyde and Acetophenone in Toluene and THF at 60 °C

		PhCHO	PhCOMe
Toluene	initial rate of catalysis (relative rate)	3.4×10^{-4} M s^{-1} (8.72)	4.82×10^{-5} M s^{-1} (1.23)
	simulated rate of catalysis (relative rate)	1.04×10^{-3} M s^{-1} (26.6)	9.7×10^{-5} M s^{-1} (2.48)
	[**1**]$_0$ mM	3.8	3.7
THF	initial rate of catalysis (relative rate)	3.6×10^{-4} M s^{-1} (9.23)	3.9×10^{-5} M s^{-1} (1)
	simulated rate of catalysis (relative rate)	4.37×10^{-4} M s^{-1} (11.2)	4.5×10^{-5} M s^{-1} (1.15)
	[**1**]$_0$ mM	6.9	6.9

Table 5. Comparison of Stoichiometric Rate Constants for Reduction of Benzaldehyde and Acetophenone by **2** in Toluene and THF at 60 °C

		PhCHO	PhCOMe
Toluene	k_3 (relative rate constant)	40 M^{-1} s^{-1} (4950)	0.43 M^{-1} s^{-1} (53.2)
THF	k_3 (relative rate constant)	7.10×10^{-2} M^{-1} s^{-1} (8.79)	8.08×10^{-3} M^{-1} s^{-1} (1)

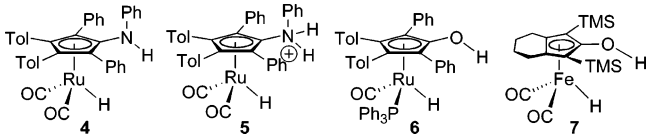

Figure 11. Catalysts designed to avoid formation of unreactive H−M−H complexes.

by the dissociation of inactive diruthenium bridging hydride **1** to the active reducing agent **2**. The slower rate of reaction of acetophenone with **2** in THF allows the build up of high concentrations of **2**.

The initial rate of acetophenone hydrogenation in THF can be predicted from direct measurement of [**2**] = 11.1 mM at 50% hydrogenation and from the rate constant for stoichiometric reduction of acetophenone by **2**: $-$d[PhCOMe]/dt = k_3[**2**][PhCOMe] = 8.08×10^{-3} M^{-1}s^{-1} [11.1×10^{-3} M][0.42 M] = 3.8×10^{-5} M^{-1}s^{-1}. This estimate is in remarkably close agreement with the experimentally observed initial rate of acetophenone hydrogenation in THF (3.9×10^{-5} M s^{-1}).

Discussion

Remarkably good agreement was found between experimental hydrogenation rates and simulated rates calculated using the reactions in Scheme 1 and rate constants extrapolated to 60 °C estimated from kinetic and equilibrium measurements made at much lower or much higher temperature (Table 4). The relative rates are presented with the slowest rate (acetophenone hydrogenation in THF) set to 1.0. This close agreement between experimental and simulated hydrogenations provides increased confidence in the fundamental soundness of the kinetic model. For example, simulated hydrogenation rates of benzaldehyde and acetophenone were only 2−3 times faster than experimental rates in toluene and only about 1.2 times faster than those in THF. The simulations also mirrored the less than first-order dependences of rates on [RCOR′], [H_2], and [**1**]$_0$, and relative rates as a function of substrate (benzaldehyde vs acetophenone) and solvent (toluene vs THF). In addition, the simulations showed similar nonequilibrium ratios of ruthenium species present during catalysis.

Scheme 1 provides an excellent qualitative (and now quantitative) picture of the kinetics of hydrogenation under a wide range of conditions. At one extreme, the hydrogenation of benzaldehyde in toluene proceeds by turnover limiting dissociation of diruthenium bridging hydride **1** to give the active reducing monoruthenium hydride reducing agent **2**, followed by hundreds of cycles in which **2** reduces benzaldehyde and generates reactive intermediate **A**, which reacts with H_2 to regenerate **2**. The reaction of **A** with H_2 occurs several hundred times faster than reaction with **2** to generate dormant diruthenium complex **1**. On each hydrogenation cycle **A** has the opportunity to be converted to **1**, and eventually this occurs. The very rapid reaction of **2** with benzaldehyde suppresses its concentration far below its equilibrium value.

In contrast, during the hydrogenation of acetophenone in THF, significant quantities of monoruthenium hydride **2** are present throughout the hydrogenation. The reaction of **2** with acetophenone in THF is much slower and occurs at a rate similar to the rate of dissociation of **1**. The slower reaction of **2** with acetophenone permits higher concentrations of **2** to develop during reaction, but [**2**] remains well below its equilibrium value until most of the acetophenone is consumed.

The kinetic model provides a deeper understanding why there are large differences in rates of stoichiometric reduction of carbonyl compounds by **2** but only small differences in hydrogenation rates. Although the stoichiometric reaction of **2** with benzaldehyde in toluene is 5000 times faster than reaction with acetophenone in THF, the catalytic hydrogenation rate is only 8.7 times faster (Table 5). Hydrogenation rates are controlled by the rate constant for stoichiometric reduction of carbonyl compound and by the concentration of the active reducing agent **2**. The leveling of hydrogenation rates results from feedback: a large rate constant for stoichiometric reaction of **2** with a carbonyl compound drives down [**2**] by providing more opportunities to be converted to **1**, the reduced concentration of [**2**] in turn moderates the rate of hydrogenation.

A distinction must be made between the kinetic model presented in Scheme 1 and the detailed mechanism of the individual reactions in the sequence. Although we have increased confidence in the kinetic model, the agreement between experimental and simulated rates provides no additional information on whether the reaction of **2** with carbonyl compounds

proceeds by an inner or outer sphere mechanism or whether an alcohol is required to mediate proton transfer in the reaction of **A** with H_2.

The Shvo catalytic system **1** ⇔ **2** often makes inefficient use of ruthenium because so much of the ruthenium is present as the dormant species **1** and so little is present as the active reducing agent **2**. To develop new more active catalysts, systems with structures that interfere with formation of unreactive M−H−M systems but maintain high reactive of the M−H species are needed (Figure 11). We successfully destabilized M−H−M formation by introducing a bulky -NHPh group on the Cp ring in place of −OH in **4**, but the low NH acidity resulted in slow stoichiometric reduction of carbonyl groups by **4**.[32] Protonation of **4** to give **5**, which possesses a much more acidic $-NH_2^+$ group, gave a very active catalyst, but acid-catalyzed side reactions led to some ether formation. Complex **6**, in which PPh_3 is substituted for one CO, also prevented formation of unreactive M−H−M complexes.[33] **6** is a very selective catalyst for hydrogenation of aldehydes over ketones; it is also a faster catalyst than **1** ⇔ **2** for aldehyde hydrogenation below 60 °C but is slower at higher temperatures. Most recently, we have discovered the economical iron catalyst **7**, which does not form M−H−M complexes and is an active catalyst for ketone hydrogenation at room temperature and 3 atm.[34] In our search for new active catalysts, we will continue to design complexes that do not form inactive M−H−M systems but have high M−H reactivity toward carbonyl compounds.

Acknowledgment. Dedicated to the memory of Professor Yoshihiko Ito. Financial support from the Department of Energy, Office of Basic Energy Sciences is gratefully acknowledged. Grants from NSF (CHE-9208463 and CHE-9709065) and NIH (1 S10 RR0 8389-01) for the purchase of NMR spectrometers are acknowledged.

Supporting Information Available: General experimental information, experimental procedures, Tables and Figures for rates of dissociation of **1**, equilibrium constants for **1** + H_2 ⇔ 2 **2**, rates of H_2 loss from **2**, rates of reduction of carbonyl compounds by **2**, and simulations of carbonyl hydrogenations from kinetic modeling. This material is available free of charge via the Internet at http://pubs.acs.org.

JA077525C

(32) Casey, C. P.; Vos, T. E.; Singer, S. W.; Guzei, I. A. *Organometallics* **2002**, *21*, 5038−5046.
(33) Casey, C. P.; Strotman, N. A.; Beetner, S. E.; Johnson, J. B.; Priebe, D. C.; Vos, T. E.; Khodavandi, B.; Guzei, I. A. *Organometallics* **2006**, *25*, 1230−1235. Casey, C. P.; Strotman, N. A.; Beetner, S. E.; Johnson, J. B.; Priebe, D. C.; Guzei, I. A. *Organometallics* **2006**, *25*, 1236−1244.
(34) Casey, C. P.; Guan, H. *J. Am. Chem. Soc.* **2007**, *129*, 5816−5817.